Elasticity and Fluctuations of Frustrated Nanoribbons

Doron Grossman,[1,*] Eran Sharon,[1,†] and Haim Diamant[2,‡]
[1]Racah Institute of Physics, Hebrew University, Jerusalem 91904, Israel
[2]Raymond and Beverly Sackler School of Chemistry, Tel Aviv University, Tel Aviv 6997801, Israel
(Received 26 November 2015; published 22 June 2016)

We derive a reduced quasi-one-dimensional theory of geometrically frustrated elastic ribbons. Expressed in terms of geometric properties alone, it applies to ribbons over a wide range of scales, allowing the study of their elastic equilibrium, as well as thermal fluctuations. We use the theory to account for the twisted-to-helical transition of ribbons with spontaneous negative curvature and the effect of fluctuations on the corresponding critical exponents. The persistence length of such ribbons changes nonmonotonically with the ribbon's width, dropping to zero at the transition. This and other statistical properties qualitatively differ from those of nonfrustrated fluctuating filaments.

DOI: 10.1103/PhysRevLett.116.258105

Slender structures appear on many scales in both natural and man-made systems. Examples vary from the tendrils and seedpods of plants [1,2], through man-made responsive gels and elastomers [3], to nanoscale structures such as graphene sheets [4] and biomolecular self-assemblies made of peptides [5], lipids [6,7], and proteins [8]. Many of these systems are frustrated in the sense that, even when free of constraints, they contain residual stresses. On the nanoscale, such frustration is particularly likely, either due to the way in which the molecular building blocks bind to one another as they self-assemble [9–11] or because of the accumulation of defects in crystalline sheets [12,13].

Present theories address the statistical-mechanical properties of compatible slender structures [14–18] and the elastic equilibrium of frustrated thin sheets (incompatible plate theory) [19–21]. In addition, a molecular model was presented for the self-assembly of chiral amphiphilic molecules into twisted ribbons [10]. There is no general theory for the combination of the two, i.e., one which models the statistical mechanics of frustrated slender structures. As indicated by the work of Ghafouri and Bruinsma [22], who modeled a specific case of a frustrated ribbon, the behavior of such systems is qualitatively different from that of ordinary semiflexible filaments.

In this Letter, we derive a general theory for the elasticity and statistical mechanics of frustrated elastic ribbons. A 1D energy functional is derived from the 2D incompatible plate theory. It describes any ribbon, irrespective of whether or not it is frustrated. Motivated by recent measurements on self-assembled supramolecular structures [11,23–25], we proceed to apply the model to a specific system possessing negative spontaneous curvature.

In the formalism of incompatible sheets [19], a 2D elastic membrane is fully described by its metric a and curvature tensor b. However, not any choice of a and b corresponds to a continuous surface in 3D Euclidean space. To form an intact surface, they must satisfy a set of geometrical constraints called the Gauss-Minardi-Patterson-Codazzi (GMPC) equations. Every elastic membrane is equipped also with two intrinsic reference fields $\bar{a}$ and $\bar{b}$. $\bar{a}$, the reference metric, encodes the preferred in-plane positions of neighboring elements, while $\bar{b}$, the reference curvature, describes the preferred orientations of these elements. In general, the reference metric and curvature may not satisfy the GMPC constraints. In such cases, the membrane is frustrated, and its configuration can usually comply with either $\bar{a}$ or $\bar{b}$, but not with both, giving rise to residual stresses.

The elastic 2D Hamiltonian of a thin elastic membrane is given by [2,19]

$$H_{2D} = \frac{Y}{8(1-\nu^2)} \iint \left(tE_s + \frac{t^3}{3} E_b \right) d^2A,$$
$$E_s = \nu \mathrm{Tr}^2[\bar{a}^{-1}(a-\bar{a})] + (1-\nu)\mathrm{Tr}[\bar{a}^{-1}(a-\bar{a})]^2,$$
$$E_b = \nu \mathrm{Tr}^2[\bar{a}^{-1}(b-\bar{b})] + (1-\nu)\mathrm{Tr}[\bar{a}^{-1}(b-\bar{b})]^2, \quad (1)$$

where E_s is the stretching content, E_b the bending content, Y Young's modulus, ν Poisson's ratio, t the thickness of the sheet (taken as the smallest length scale in the system), and $d^2A = \sqrt{\det \bar{a}}\, du\, dv$ the surface element (u and v being a coordinate system on the sheet).

We consider a long (length L), narrow (width W), and thin (thickness t) ribbon, such that $t \ll W \ll L$. We select a preferable set of coordinates $(x, y) \in [0, L] \times [-(W/2), (W/2)]$, such that the midline of the ribbon is given by $(x, 0)$. As a first step, we reduce Eq. (1) into a 1D Hamiltonian through an expansion of the curvatures around the midline in small y (compared to the typical radius of curvature). While performing the expansion, we make sure that a and b continue to describe an intact surface—i.e., that they satisfy the GMPC constraints up to the appropriate order. Only after this self-consistency is established do we allow the system to find the preferred configuration.

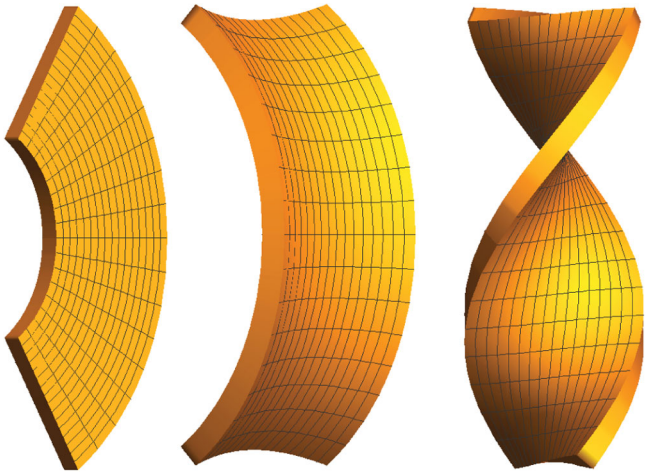

FIG. 1. Geometric interpretation of the different curvatures. Left to right: κ_g, l and n (opposite signs), m.

Let us consider a ribbon, cut off an elastic membrane with the reference $\bar{a}$ and $\bar{b}$, and zoom in on an indefinitely narrow strip around its midline. The deformation of such a strip can be parametrized by four local curvatures, (κ_g, l, m, n), whose geometrical meanings are illustrated in Fig. 1, and a Gaussian curvature K. In particular, κ_g is the geodesic curvature of the midline. These curvatures may vary along the midline; i.e., they all may be functions of x. The reference metric and curvature of the original membrane impart to these functions a reduced-1D reference state $(\bar{\kappa}_g, \bar{l}, \bar{m}, \bar{n})$ and $\bar{K}$. For a sufficiently narrow ribbon [specifically, $W \ll (1/\bar{\kappa}_g, 1/\sqrt{\bar{K}})$], we may expand in small distance y perpendicular to the midline and obtain the following relation between the 2D and reduced-1D references:

$$\bar{a} = \begin{pmatrix} (1+\bar{\kappa}_g y)^2 - \bar{K}y^2 + O(y^3) & 0 \\ 0 & 1 \end{pmatrix},$$

$$\bar{b} = \begin{pmatrix} \bar{l} & \bar{m} \\ \bar{m} & \bar{n} \end{pmatrix} + O(y).$$

While the reference tensors $(\bar{a}, \bar{b})$ are arbitrary, the *actual* metric and curvature tensors of a given configuration must satisfy the GMPC equations. A self-consistent expansion of these tensors gives [26]

$$a = \begin{pmatrix} (1+\bar{\kappa}_g y)^2 - (ln - m^2)y^2 & 0 \\ 0 & 1 \end{pmatrix} + O(y^2), \quad (2a)$$

$$b = \begin{pmatrix} l + m'y & m + n'y \\ m + n'y & n \end{pmatrix} + O(y), \quad (2b)$$

where a prime denotes a derivative with respect to x, and we have set $\kappa_g = \bar{\kappa}_g$, since it is easily shown that deviations from this equality are too costly energetically. Inserting the expressions for a, b, $\bar{a}$, $\bar{b}$ in the 2D Hamiltonian (1) and integrating over the narrow coordinate y, we end up with a reduced-1D Hamiltonian

$$\begin{aligned} H_{1D} = \frac{Y}{8(1-\nu^2)} \int dx \Big\{ & \frac{1}{80} t W^5 (\bar{K} - ln + m^2)^2 \\ & + \frac{1}{3} t^3 W \Big[2(1-\nu) \Big(\frac{W^2}{12} (n')^2 \\ & - [(\bar{l} - l)(\bar{n} - n) - (\bar{m} - m)^2] \Big) \\ & + (\bar{l} + \bar{n} - n - l)^2 + \frac{W^2}{12} (m')^2 \Big] \Big\}. \end{aligned} \quad (3)$$

Equation (3) is the central result of the present work, providing the energy functional for a wide range of nonfrustrated as well as frustrated ribbons. The quasi-1D reduction significantly simplifies the problem, allowing for an analytical solution in simple cases (such as the one treated below) and the study of thermal fluctuations around the minimum.

Equation (3) is considerably simplified when applied to specific ribbons, or under some common approximations such as that of an unstretchable ribbon. This limit holds when the stretching rigidity is much larger than the bending rigidity, as in the limit of vanishing thickness. It implies $a = \bar{a}$, leading to elimination of the first integral. If, in addition, we consider the case with no spontaneous curvature, i.e., $\bar{K} = \bar{\kappa}_g = \bar{l} = \bar{m} = \bar{n} \equiv 0$, we recover the known Sadowsky functional [27–29]

$$\begin{aligned} H &= \frac{Y}{8(1-\nu^2)} \int \Big[\frac{1}{3} t^3 W (l+n)^2 \Big] dx \\ &= \frac{Y t^3 W}{24(1-\nu^2)} \int \frac{(\kappa^2 + \tau^2)^2}{\kappa^2} dx. \end{aligned} \quad (4)$$

We now use the 1D Hamiltonian of Eq. (3) to provide an analytic description for the system described in Ref. [25]. This is the case of a flat in-plane geometry (i.e., Euclidean $\bar{a}$) $\bar{K} = 0$ and spontaneous twist along the x direction (which implies a saddle curvature) $\bar{l} = \bar{n} = 0$, $\bar{m} = k_0$. Such intrinsic geometry commonly appears in nanoribbons generated by the self-assembly of chiral molecules. These include lipids [30], peptides [5], and proteins that form amyloids [31]. The corresponding reference tensors are

$$\bar{a} = \begin{pmatrix} 1 & 0 \\ 0 & 1 \end{pmatrix}, \qquad \bar{b} = \begin{pmatrix} 0 & k_0 \\ k_0 & 0 \end{pmatrix}. \quad (5)$$

The Hamiltonian of this specific system, omitting small derivatives, is given by

$$H = \frac{Y}{8(1-\nu^2)} \int \left\{ \frac{1}{80} t W^5 (ln - m^2)^2 + \frac{1}{3} t^3 W \{ (l+n)^2 - 2(1-\nu)[ln - (k_0 - m)^2] \} \right\} dx. \tag{6}$$

The equilibrium configuration is found by solving the appropriate Euler-Lagrange equations [26]. By defining dimensionless parameters $\tilde{w} = W/W^*$, $\tilde{\sigma} = \sigma_i/k_0 (\sigma_i \in \{l, m, n\})$, where $W^* = \{[320(1+\nu)]/[3(1-\nu)^2](t^2/k_0^2)\}^{1/4}$, the solution gets the nifty form

$$\tilde{n} = \tilde{l} = \begin{cases} 0 & \tilde{w} \le 1 \\ \pm \frac{1}{2}(1-\nu)\frac{\sqrt{\tilde{w}^4 - 1}}{\tilde{w}^2} & \tilde{w} > 1, \end{cases} \tag{7a}$$

$$\tilde{m} = \begin{cases} \frac{1}{2}(1-\nu)\frac{[\tilde{\Xi}^2(\tilde{w}) - (1-\nu^2)3^{1/3}]}{3^{2/3}(1+\nu)\tilde{\Xi}(\tilde{w})\tilde{w}^2} & \tilde{w} \le 1 \\ \frac{1}{2}(1-\nu) & \tilde{w} > 1, \end{cases}$$
$$\tilde{\Xi}(\tilde{w}) = \left[\sqrt{[81(1+\nu)^4\tilde{w}^4 + 3(1-\nu^2)^3]} + 9(1+\nu)^2\tilde{w}^2\right]^{1/3}. \tag{7b}$$

We compare in Fig. 2 the resulting dimensionless pitch and radius of the midline $\tilde{P} = (1-\nu)k_0(2\pi m/m^2 + l^2)$, $\tilde{R} = (1-\nu)k_0(l/m^2 + l^2)$, with the solution obtained by 2D finite element numerics. Both describe a ribbon that changes its shape from twisted to helical as it widens.

Equations (7) describe a continuous (second order) transition, at $W = W^*$ ($\tilde{w} = 1$), which separates two regimes: bending dominated (i.e., minimization of the bending content is favored) and stretching dominated (in which the solution of the bending-dominated regime is unstable). The $\pm$ signs mark a spontaneous symmetry breaking obtained by flipping a helix inside out (while preserving chirality). The twist-to-helical transition was observed in experiments and simulations [2,3,32], and the scaling of the critical width and existence of these two regimes were estimated in Ref. [2]. Qualitatively similar results were obtained within a modified 1D worm-like-chain model [22]. We use this example to mainly underline the strength of the general formalism presented here. In addition, the explicit solution, obtained from a controlled approximation of the 2D elastic problem, allows us to safely proceed to study in detail the statistical properties of the ribbons, on both sides of the transition.

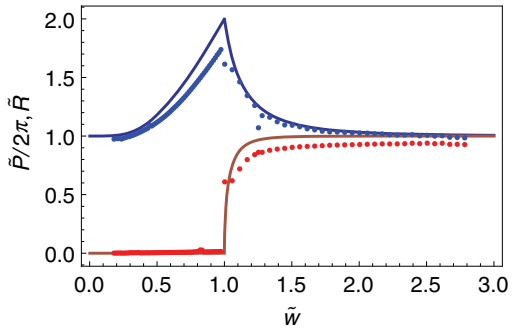

FIG. 2. Pitch (upper curve) and radius (lower curve) of the ribbon as a function of its width, as obtained from the analytical 1D model (solid lines) and 2D simulations (circles).

The nature of the elastic transition (Fig. 2) is captured by its critical exponents, denoted by the conventional symbols $\alpha, \beta, \gamma, \delta, \nu_w, \eta$ [33]. The control parameter of the transition is the ribbon's width $\tilde{w}$. Noting that the most singular behavior is exhibited by the mean curvature $\tilde{\Omega} \equiv \frac{1}{2}(\tilde{l} + \tilde{n})$, we readily find the critical exponents [26]: $\alpha = 0$, $\beta = \frac{1}{2}$, $\gamma = 1$, $\delta = 3$.

We now turn to thermal fluctuations of the ribbon around its ground state. These affect various observable properties of nanoribbons, such as the distributions of radius and pitch, as well as the persistence length characterizing the bending fluctuations of the entire ribbon as a polymerlike object [34]. We expand the Hamiltonian (3) around its equilibrium values to second order in the fluctuations $\Delta\sigma_i (\sigma_i \in \{l, m, n\})$, so that

$$H = H_{\rm eq} + \int \mathcal{H}_{ij}^{(2)} \Delta\sigma_i \Delta\sigma_j dx, \tag{8}$$

where $H_{ij}^{(2)} = (\partial^2 H/\partial\sigma_i \partial\sigma_j)$, and we adopt the summation convention. Transforming to Fourier space ($x/W^* \to q$), and keeping only leading contributions near the transition, we obtain $H - H_{\rm eq} \propto \int (A_\pm |\delta\tilde{w}| + B_\pm q^2) |\Delta\tilde{\Omega}|^2 dq$, where $A_\pm$, $B_\pm$ are positive constants with different values below ($-$) and above ($+$) the transition [26]. This calculation leads to the modified (but expected) values of exponents: $\alpha = \frac{3}{2}$, $\nu_w = \frac{1}{2}$, $\eta = 0$, while β, γ, δ remain unchanged. Because of the one-dimensionality of the Hamiltonian, the critical exponent α has an atypical value. It is readily verified that the hyperscaling relation $2 - \alpha = \nu_w d$ is satisfied with $d = 1$.

Calculating the fluctuations of the pitch and radius, within the Gaussian approximation, and integrating out Δn, we have

$$\langle \Delta\tilde{P}^2 \rangle = \frac{k_B T}{L Y k_0^{3/2} t^{7/2}} \tilde{\mathcal{H}}_{pp}^{-1}, \tag{9a}$$

$$\langle \Delta\tilde{R}^2 \rangle = \frac{k_B T}{L Y k_0^{3/2} t^{7/2}} \tilde{\mathcal{H}}_{rr}^{-1}, \tag{9b}$$

$$\langle \Delta\tilde{P}\Delta\tilde{R} \rangle = \frac{k_B T}{L Y k_0^{3/2} t^{7/2}} \tilde{\mathcal{H}}_{rp}^{-1}, \tag{9c}$$

where $\tilde{\mathcal{H}}$ is the dimensionless Hamiltonian. The functions $\tilde{\mathcal{H}}_{ij}^{-1}$ are shown in Fig. 3(a) as a function of $\tilde{w}$ [26].

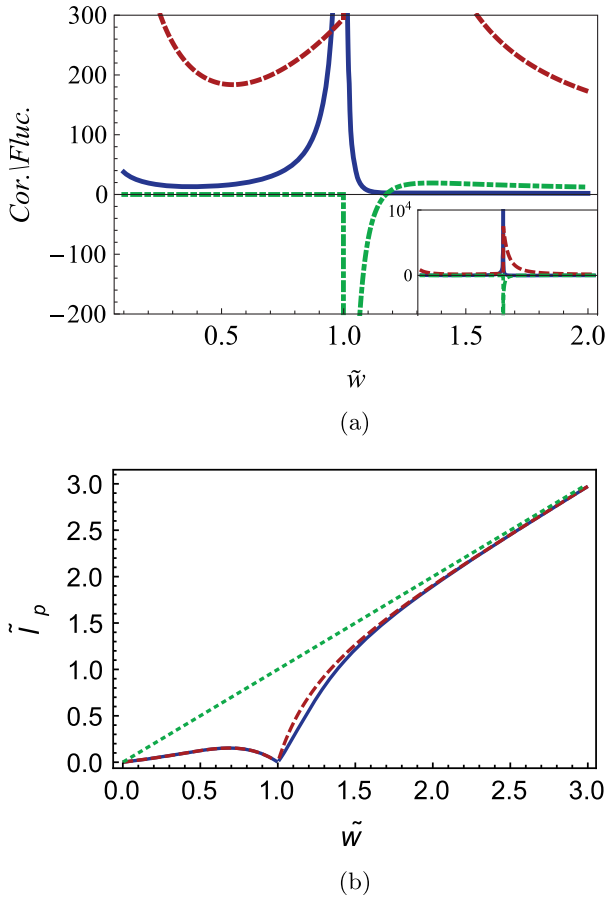

FIG. 3. (a) Correlations and fluctuations as a function of ribbon width, in the case of $\nu = 0$. $\tilde{\mathcal{H}}_{rr}^{-1}$ is a solid blue line, $\tilde{\mathcal{H}}_{rp}^{-1}$ is a dash-dotted green line, and $\tilde{\mathcal{H}}_{pp}^{-1}$ is a dashed red line. Inset: zoomed out view. Note that fluctuations in $\tilde{P}$ are finite (though discontinuous). For $\nu \neq 0$, features remain the same, although values vary. (b) Normalized persistence length $\tilde{l}_p = (3(1-\nu^2)/2)(k_BT/Yt^3W^*)l_p$, for different temperatures: $(k_BT/Yt^3W^*) = 0.01$ (solid blue line) and 100 (dashed red line). The dotted green line shows the asymptote $\tilde{l}_p = \tilde{w}$.

At the critical width, the fluctuations of the radius diverge due to the existence of an infinitely soft mode. Including the spatial (q) dependence of the fluctuations is important, as it changes the divergence from $|\tilde{w}-1|^{-1}$ ($q = 0$ case) to $|\tilde{w}-1|^{-1/2}$. Right above the transition ($\tilde{w} > 1$), the pitch and radius are negatively correlated (i.e., changes in the radius usually occur with an opposite change in the pitch). As the ribbon widens, the correlations change sign to become positive. This implies a change in the nature of the system's eigenmodes, which leads to the following testable prediction: Close to W^*, thermal fluctuations induce strong winding (under extension) and unwinding (under compression) of the ribbons. Away from W^*, the trend changes and thermal fluctuations induce unwinding (under extension).

Having analyzed the fluctuations, we can calculate the persistence length, characterizing the bending fluctuations of the ribbon as an effective 1D polymer $l_p = \lim_{L\to\infty}(1/2L)\langle|\vec{r}|^2\rangle$, where $\vec{r}$ is the ribbon's end-to-end vector. This is a commonly measured quantity in polymer solutions, either on the level of a single molecule or on the ensemble level using scattering. Intuitively, one expects the stiffness of the midline, and therefore l_p, to increase with the ribbon width, as indeed is found in nonfrustrated ribbons [18]. Using the same formalism as in Ref. [35], we find that the persistence length is nonmonotonic in the width; see Fig. 3(b). Instead of continually increasing, it drops to 0 at the critical width. We find that near the transition,

$$l_p = C_\pm\sqrt{|\tilde{w}-1|},$$

where $C_\pm$ are different positive constants below and above the transition. Again, this result crucially depends on the integration over all fluctuation wave vectors q (yielding an exponent of $1/2$ instead of 1). Far above the transition, asymptotically, we have

$$l_p \overset{\tilde{w}\gg 1}{\longrightarrow} \frac{2}{3}\frac{Yt^3}{k_BT}\frac{W^*}{(1-\nu^2)}\tilde{w}.$$

This value is much larger than the one found for equivalent nonfrustrated ribbons and is a direct consequence of the frustration. The fluctuation ribbon has additional geometrical correlations, such as the torsional (normal-normal), normal-binormal, and normal-tangent correlations, all exhibiting decaying oscillations (not shown).

We conclude with a few possible implications of our results for future experiments. The pitch and radius associated with the twist-to-helical transition (Fig. 2) were measured in macroscopic systems [2]. These observables can be measured also in nanometric systems such as the self-assembled peptide ribbons of Refs. [5,9,10,36]. The former work was limited to narrow ribbons below the transition, while in the latter, the transition was only qualitatively characterized. Our work provides quantitative predictions regarding the statistical nature of thermal ribbons—specifically, the fluctuations in pitch and radius, and their correlations, and the persistence length of the ribbon's axis. The pitch and radius may be observed using electron microscopies [11,23]. The persistence length and its anomalous dependence on the ribbon's width can be measured using light scattering. In particular, our theory predicts that, close to the transition, the persistence length should become very small. Under these conditions, long ribbons should behave as random coils. The properties of a suspension of such ribbons should qualitatively change and resemble a solution of flexible polymers [37].

We expect the results presented here, in particular, the reduced Hamiltonian of Eq. (3), to be relevant to a range of biological, chemical, and condensed matter systems, in which fluctuating frustrated ribbons are known to exist.

The authors thank Y. Kantor for a helpful comment and The Jacob Blaustein Institutes for Desert Research for their hospitality. E. S. and D. G. were supported by the European Research Council SoftGrowth project. D. G. was also supported by The Harvey M. Kruger Family Center of Nanoscience and Nanotechnology.

*doron.grossman@mail.huji.ac.il
†erans@mail.huji.ac.il
‡hdiamant@tau.ac.il

[1] S. J. Gerbode, J. R. Puzey, A. G. McCormick, and L. Mahadevan, Science **337**, 1087 (2012).
[2] S. Armon, E. Efrati, R. Kupferman, and E. Sharon, Science **333**, 1726 (2011).
[3] Y. Sawa, F. Ye, K. Urayama, T. Takigawa, V. Gimenez-Pinto, R. L. B. Selinger, and J. V. Selinger, Proc. Natl. Acad. Sci. U.S.A. **108**, 6364 (2011).
[4] J. C. Meyer, A. K. Geim, M. Katsnelson, K. Novoselov, T. Booth, and S. Roth, Nature (London) **446**, 60 (2007).
[5] L. Ziserman, H.-Y. Lee, S. R. Raghavan, A. Mor, and D. Danino, J. Am. Chem. Soc. **133**, 2511 (2011).
[6] B. N. Thomas, C. M. Lindemann, and N. A. Clark, Phys. Rev. E **59**, 3040 (1999).
[7] A. Singh, E. M. Wong, and J. M. Schnur, Langmuir **19**, 1888 (2003).
[8] C. Lara, J. Adamcik, S. Jordens, and R. Mezzenga, Biomacromolecules **12**, 1868 (2011).
[9] A. Aggeli, M. Bell, N. Boden, J. Keen, P. Knowles, T. McLeish, M. Pitkeathly, and S. Radford, Nature (London) **386**, 259 (1997).
[10] A. Aggeli, I. Nyrkova, M. Bell, R. Harding, L. Carrick, T. McLeish, A. Semenov, and N. Boden, Proc. Natl. Acad. Sci. U.S.A. **98**, 11857 (2001).
[11] R. Oda, I. Huc, M. Schmutz, S. J. Candau, and F. C. MacKintosh, Nature (London) **399**, 566 (1999).
[12] V. B. Shenoy, C. D. Reddy, A. Ramasubramaniam, and Y. W. Zhang, Phys. Rev. Lett. **101**, 245501 (2008).
[13] P. Koskinen, S. Malola, and H. Häkkinen, Phys. Rev. B **80**, 073401 (2009).
[14] D. Nelson, T. Piran, and S. Weinberg, *Statistical Mechanics of Membranes and Surfaces*, Jerusalem Winter School for Theoretical Physics Vol. 5 (World Scientific, Singapore, 1989).
[15] C. Bouchiat and M. Mézard, Phys. Rev. Lett. **80**, 1556 (1998).
[16] T. B. Liverpool, R. Golestanian, and K. Kremer, Phys. Rev. Lett. **80**, 405 (1998).
[17] S. Panyukov and Y. Rabin, Phys. Rev. Lett. **85**, 2404 (2000).
[18] L. Giomi and L. Mahadevan, Phys. Rev. Lett. **104**, 238104 (2010).
[19] E. Efrati, E. Sharon, and R. Kupferman, J. Mech. Phys. Solids **57**, 762 (2009).
[20] E. Efrati, E. Sharon, and R. Kupferman, Phys. Rev. E **80**, 016602 (2009).
[21] E. Efrati, E. Sharon, and R. Kupferman, Phys. Rev. E **83**, 046602 (2011).
[22] R. Ghafouri and R. Bruinsma, Phys. Rev. Lett. **94**, 138101 (2005).
[23] L. Ziserman, A. Mor, D. Harries, and D. Danino, Phys. Rev. Lett. **106**, 238105 (2011).
[24] J. Adamcik, J.-m. Jung, J. Flakowski, P. De Los Rios, G. Dietler, and R. Mezzenga, Nat. Nanotechnol. **5**, 423 (2010).
[25] S. Armon, H. Aharoni, M. Moshe, and E. Sharon, Soft Matter **10**, 2733 (2014).
[26] See Supplemental Material at http://link.aps.org/supplemental/10.1103/PhysRevLett.116.258105 for the detailed calculations.
[27] M. Sadowsky, Sitzungsber. Preuss. Akad. Wiss. Phys. Math. Kl. **22**, 412 (1930).
[28] W. Wunderlich, Monatshefte für Mathematik **66**, 276 (1962).
[29] The last equality was derived by solving for n from the relation (Gauss' theorema egregium) $nl - m^2 = 0$ for a Euclidean membrane, and setting $l = \kappa$, $m = \tau$ in accordance with the Frenet-Serret frame.
[30] B. N. Thomas, C. R. Safinya, R. J. Plano, and N. A. Clark, Science **267**, 1635 (1995).
[31] J. Adamcik and R. Mezzenga, Macromolecules **45**, 1137 (2012).
[32] R. L. B. Selinger, J. V. Selinger, A. P. Malanoski, and J. M. Schnur, Phys. Rev. Lett. **93**, 158103 (2004).
[33] P. M. Chaikin and T. C. Lubensky, *Principles of Condensed Matter Physics* Vol. 1 (Cambridge University Press, Cambridge, England, 2000).
[34] We have made sure that the corresponding functional integration maintains the correct measure [38–40].
[35] S. Panyukov and Y. Rabin, Phys. Rev. E **62**, 7135 (2000).
[36] I. Nyrkova, A. Semenov, A. Aggeli, M. Bell, N. Boden, and T. McLeish, Eur. Phys. J. B **17**, 499 (2000).
[37] M. Rubinstein and R. H. Colby, *Polymer Physics* (Oxford University Press, Oxford, England, 2003).
[38] W. Cai, T. Lubensky, P. Nelson, and T. Powers, J. Phys. II (France) **4**, 931 (1994).
[39] L. Giomi and L. Mahadevan, Phys. Rev. Lett. **107**, 239802 (2011).
[40] E. L. Starostin and G. H. M. van der Heijden, Phys. Rev. Lett. **107**, 239801 (2011).